

AMMRC TR 70-16

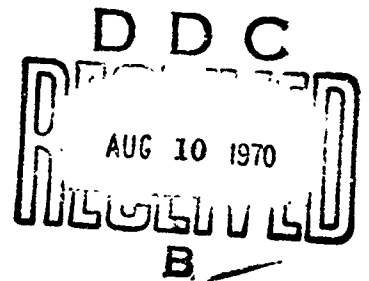
AD

AD 709602

DYNAMIC RESPONSE OF A
CONSTRAINED FIBROUS SYSTEM
SUBJECTED TO TRANSVERSE IMPACT
Part II - A MECHANICAL MODEL

FRANCIS deS. LYNCH
FIBERS AND POLYMERS DIVISION

July 1970



This document has been approved for public release and sale; its distribution is unlimited.

ARMY MATERIALS AND MECHANICS RESEARCH CENTER
Watertown, Massachusetts 02172

22

ADDRESS		
POST	WHITE SECTION	<input type="checkbox"/>
DATE	BLUE SECTION	<input type="checkbox"/>
TIME		<input type="checkbox"/>
GASTR BUTION AVAILABILITY CODES		
DIST.	AVAIL.	SPECIAL
/		

The findings in this report are not to be construed as an official Department of the Army position, unless so designated by other authorized documents.

Mention of any trade names or manufacturers in this report shall not be construed as advertising nor as an official indorsement or approval of such products or companies by the United States Government.

DISPOSITION INSTRUCTIONS

Destroy this report when it is no longer needed.
Do not return it to the originator.

AMMRC TR 70-16

**DYNAMIC RESPONSE OF A CONSTRAINED FIBROUS SYSTEM SUBJECTED TO
TRANSVERSE IMPACT. Part II. A MECHANICAL MODEL**

Technical Report by
FRANCIS deS. IYNCH

July 1970

D/A Project 1T062105A329
AMCMS Code 502E.11.295
Organic Materials Research for Army Materiel
Agency Accession Number DA OB4752

This document has been approved for public release and sale; its distribution is unlimited.

FIBERS AND POLYMERS DIVISION
ARMY MATERIALS AND MECHANICS RESEARCH CENTER
Watertown, Massachusetts 02172

ARMY MATERIALS AND MECHANICS RESEARCH CENTER

DYNAMIC RESPONSE OF A CONSTRAINED FIBROUS SYSTEM
SUBJECTED TO TRANSVERSE IMPACT

PART II: A MECHANICAL MODEL

ABSTRACT

A "finite element" mechanical model, capable of utilizing experimentally determined material properties, is presented for analyzing the deformation processes in a finite, constrained flexible filament subjected to transverse impact.

The model is then used to analyze the results of experimentally (transversely) impacted finite lengths of nylon yarns rigidly clamped at both ends. The experimental analysis is presented in Part I of this work.

The analysis is used to determine the effects of an elastic foundation transversely supporting a flexible filament subjected to transverse impact.

Finally, results of a finite element analysis of a transversely impacted isotropic membrane are presented to indicate the direction for future research.

An appendix is attached which demonstrates the ability to include rate-dependent material properties in the analyses described above.

CONTENTS

	Page
ABSTRACT	
INTRODUCTION	1
SUMMARY OF EXPERIMENTAL RESULTS (PART I)	1
THE METHOD OF ANALYSIS	
Background	3
Procedure	3
Elastic Foundation	5
Membrane Analysis	5
RESULTS OF THE ANALYSIS	
Transverse Impact of Linear Elastic Filament	7
Explanation of Experimental Results for Projectile Energy Loss . .	7
Impact of Filament With Nonlinear Material Properties	10
Impact of Filament on an Elastic Foundation	10
Transverse Impact of a Flexible Membrane	11
CONCLUSIONS	12
APPENDIX. LINEAR VISCOELASTIC EFFECTS	13
LITERATURE CITED	15

INTRODUCTION

The transient deformation of constrained fibrous systems subjected to high-speed transverse impact is being studied to gain a better understanding of the performance of textile and felt materials used for armor systems. A description of the experimental portion of this program is given in Part I of this investigation.¹ Although there has been fairly extensive research into the properties of individual, unconstrained fiber components with transverse impact at ballistic velocities,²⁻⁵ there has been a singular deficiency in defining how these properties translate into the system behavior, i.e., the constrained fiber including the boundary interactions. The missing ingredient has been a mechanical model which can utilize the fiber properties obtained from a tractable experiment to predict the behavior of the system under practical conditions. This is essential both for the evaluation of meaningful armor test conditions and to understand the performance of the fiber under in-use conditions as a component of an armor system.

A summary of the experimental program in Part I of this work¹ is given below. The "finite element" mechanical model is then developed and used to predict and analyze the experimental results obtained for the simple constrained fiber system. More practical constraints are then applied to demonstrate the ability to perform the analysis for diverse physical situations. These include the effects of an elastic foundation resisting deformation and the impact of an isotropic membrane.

An appendix is attached which demonstrates the ability to include rate-dependent material properties in the models described above.

SUMMARY OF EXPERIMENTAL RESULTS

The experimental program detailed in Part I of this work¹ was developed for obtaining fiber properties under impact conditions and studying how a simple constrained system using these fibers would behave. Figures 1 and 2 illustrate the type of results obtained from this experimental program.

Figure 1 is a photograph taken with several flash exposures indicating the gross deformation caused by a missile transversely impacting the constrained system of a low-tenacity nylon yarn bundle rigidly fixed at both ends. There is symmetry about the point of impact; therefore, only the upper half of the yarn bundle is shown. From results such as these, for very short times after impact, before the deformation processes interact with the boundaries, a dynamic stress-strain curve can be obtained for the fibers.⁴ This stress-strain curve will be some average value over the rates involved in obtaining the data; the true viscoelastic relationships are considered in Reference 5 and the appendix. For longer times after impact, after at least one reflection of the transverse displacement wave, an "average" stress-strain curve over somewhat lower rates may be obtained.³

Figure 2 is a plot of the energy lost by the projectile, which impacts and breaks the constrained fiber system, as a function of the impact velocity. The energy is expressed per unit mass of the fiber between the clamps.

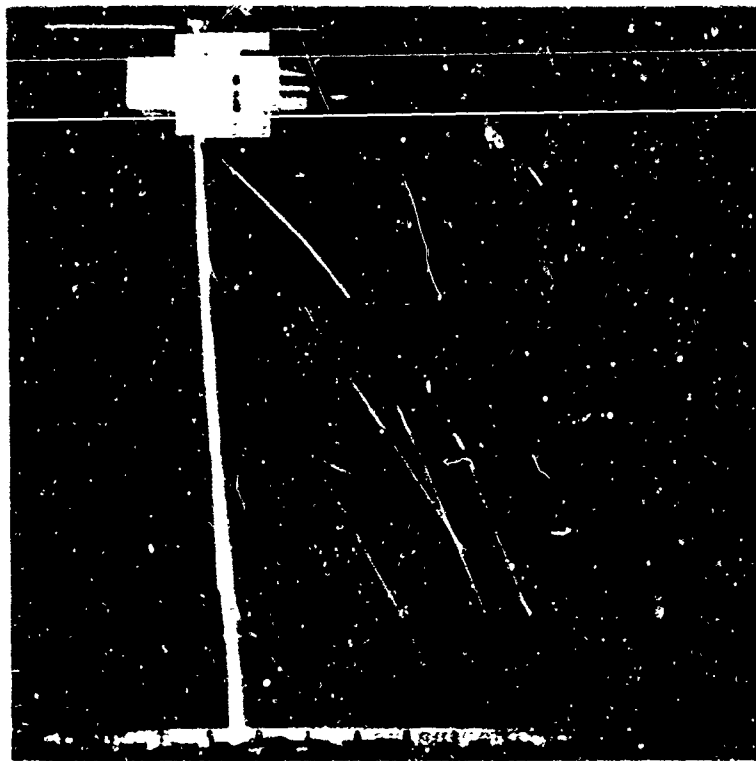


Figure 1. TYPICAL PHOTOGRAPH OF IMPACTED YARN BUNDLE SHOWING DEFORMATION AND RUPTURE. Bundle contains 4 yarns of low tenacity nylon 6/6. Impact velocity 341 feet per second. Time of 325 microseconds between flash exposures.

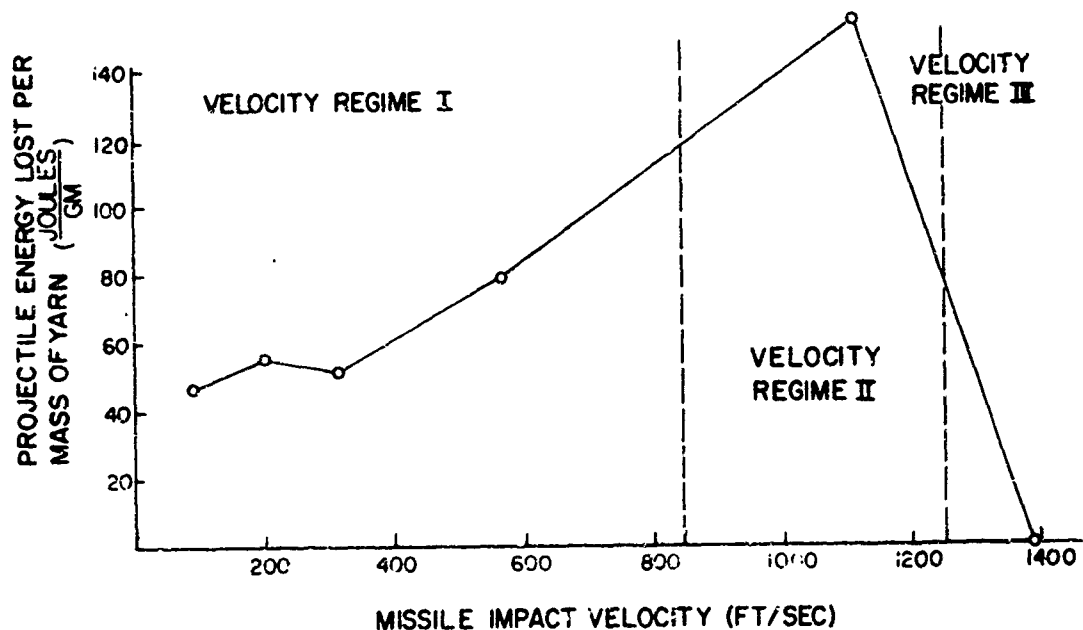


Figure 2. ENERGY STORED IN HIGH TENACITY NYLON FIBER SYSTEM VERSUS TRANSVERSE IMPACT VELOCITY.¹ Velocity regime I: quasi-static fiber response negligible wave propagation effects; material properties from method in Ref. 3. Velocity regime II: dynamic fiber-system response, important wave-boundary interactions; material properties from method in Ref. 4. Velocity regime III: dynamic fiber response rate-dependent considerations become important and boundary effects are negligible.

It is now necessary to develop a mechanical model in order to explain how the basic fiber properties, which can be obtained as mentioned above, translate into the fiber system behavior indicated in Figures 1 and 2.

THE METHOD OF ANALYSIS

Background

The mechanical model, which appears to satisfy the requirements for analyzing constrained fibrous systems, is a modification of the "direct analysis" of waves in elastic media developed by Mehta, Koenig, and Davids.^{6,7}

The modeling and subsequent "direct analysis" using physical laws in an incremental form, rather than differential equations, constitute what has become known as "finite element" analysis. In conventional mathematical procedures, differential equations are derived from the physical laws and an attempt is then made to solve these equations subject to appropriate initial conditions and boundary conditions. For problems as complex as those considered here, the differential equations must be solved by numerical methods, and even then the numerical techniques are often quite complex and may not be tractable.

In the finite element analysis the differential equations are regarded as dispensable and the physical laws are used directly to effect changes in the system that adhere to these laws (e.g., conservation of energy, momentum-impulse balance, and material constitutive laws).

The main advantages of this analysis are that it is easier to model the physics of the problem, i.e., system constraints, and experimentally measured or observable behavior, and the subsequent numerical procedure is more direct and efficient.

Procedure

The procedure follows the development of Koenig and Davids.⁷

The fiber system is divided into finite lengths (ΔL) of flexible (i.e., no shear or bending rigidity) filament (see Figure 3). The physical laws are then written in incremental form for a typical finite element:

The impulse-momentum balance, relating the velocity vector (\bar{V}) and tension per lineal density (T/m) over an increment of time (Δt) is

$$\Delta \bar{V}(j+1) = \frac{T(j+1) - T(j)}{m(j+1)\Delta L} \Delta t. \quad (1)$$

The strain (ϵ) - velocity relationship is

$$\Delta \epsilon(j) = \frac{\bar{V}(j+1) - \bar{V}(j)}{\Delta L} \Delta t \quad (2)$$

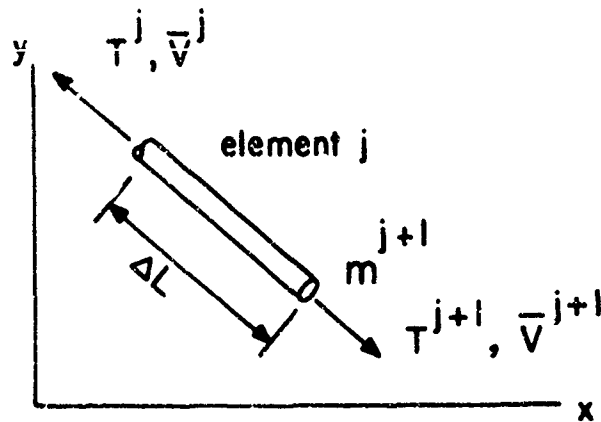


Figure 3. TYPICAL FINITE FLEXIBLE ELEMENT

The tension (per lineal density) - strain constitutive law utilizing the modulus per lineal density (E) is

$$\frac{\Delta T(j)}{m(j)} = E[\epsilon(j)] \cdot \Delta \epsilon(j). \quad (3)$$

Equations (1), (2), and (3) completely state the problem of traveling waves, in a bounded, elastic, ideally flexible filament, when combined with appropriate boundary conditions. These formulations may be used directly in a computer code.

In order to insure stability of the calculations it is convenient to define the element size-time increment relation which conserves energy in the propagation of the leading wave disturbance (in this case, longitudinal elastic waves propagating at the velocity $C_0 = (E_0)^{1/2}$, where E_0 is the modulus per lineal density (e.g., grams per denier) of the steepest portion of the tension-strain curve):

$$\Delta t \geq \Delta L / C_0.$$

The element size is arbitrary, yet assures that a further reduction in size will not yield any significant change in the resulting solution of the problem.

The boundary conditions and physical parameters are specified; then equations (1) - (3) are applied sequentially to each element from the impact point to the boundary for one increment of time. This step is repeated to yield an accumulated solution after each further increment of time.

It should be noted that no specific operations are required to deal with reflected waves. The reflected longitudinal waves are automatically generated simply by specifying the appropriate boundary conditions. Similarly, transverse deflection waves are automatically generated in order that the system response adheres to the governing physical laws.

Elastic Foundation

In order to simulate the effect of the support which the human body provides for a simple fiber system, a transverse resistive force (R) is applied to the filament proportional to the transverse displacement (y), $R = Ky$. Similarly, air drag, $R = D \cdot \Delta y / \Delta t$, or other such forces could easily be added without increasing the complexity of the analysis.

Membrane Analysis

As a further step in simulating how more practical fibrous systems behave, a finite element model for the transverse impact of an isotropic membrane (a first approximation to a sheet of fabric) is now developed.

The membrane is divided into finite semi-annuli as shown in Figure 4. The physical laws are then written in incremental form for a typical finite element. The treatment of cylindrical elastic waves in Reference 6 follows a similar development to the following.

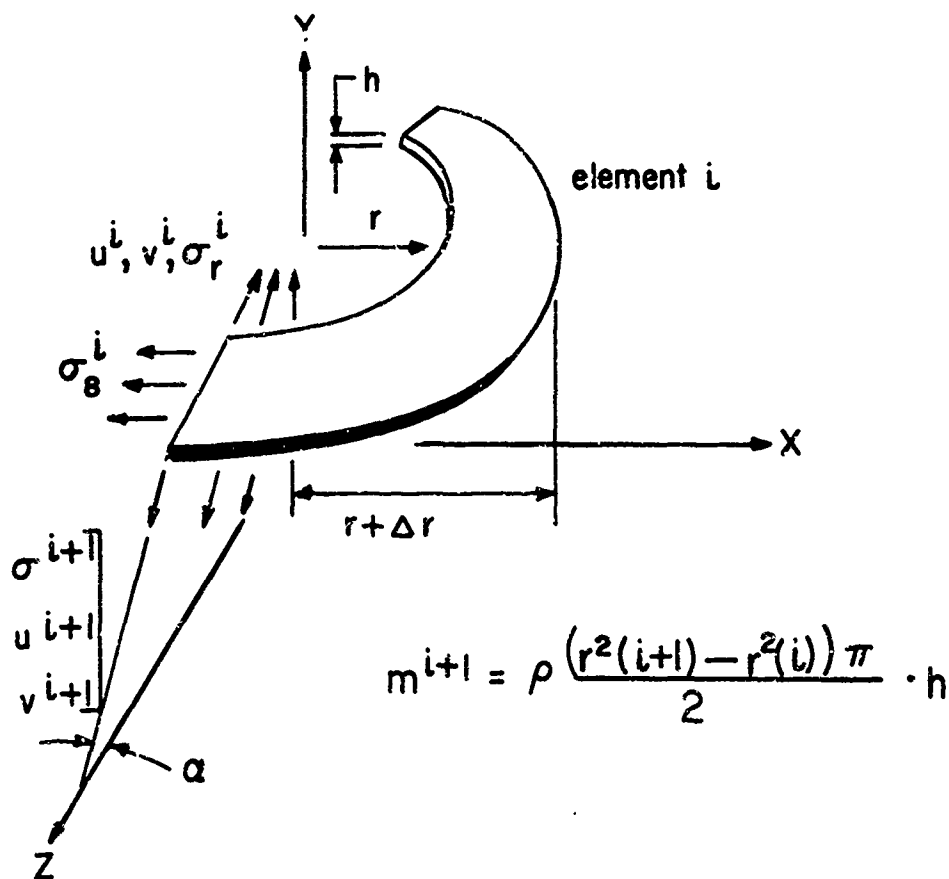


Figure 4. TYPICAL FINITE FLEXIBLE MEMBRANE ELEMENT

The impulse-momentum balance relating the particle velocities (u,v) in the r,y directions, the radial (σ_r) and circumferential stresses (σ_θ) and the density (ρ) per unit volume are derived by first considering the motion of the center of gravity of the semi annulus [$V_x(C.G.)$, $V_y(C.G.)$] in the x and y directions, caused by the net forces ($\sum F_x$, $\sum F_y$) in these directions:

$$\begin{aligned} m(i) \cdot \Delta V_y(C.G.) &= \sum F_y \Delta t, \\ m(i) \cdot \Delta V_x(C.G.) &= \sum F_x \Delta t. \end{aligned}$$

The velocities of the center of gravity must now be related to the element particle velocities. The element moving from radial position r to $r+\Delta r$ has its center of gravity moved from $\frac{2r}{\pi}$ to $\frac{2(r+\Delta r)}{\pi}$ in time Δt therefore $\Delta V_x(C.G.) = \frac{2}{\pi} \frac{\Delta r}{\Delta t}$. But, the particles along a radius of the element move from r to $r+\Delta r$ therefore, $\Delta u = \frac{\Delta r}{\Delta t}$. The relation between the particle velocity in the r-direction and the center of gravity motion in the x-direction becomes $\Delta u = \frac{\pi}{2} \Delta V_x(C.G.)$. The particle velocity in the y-direction is identical to the velocity of the center of gravity in the y-direction, $\Delta v = \Delta V_y(C.G.)$.

Therefore, the impulse-momentum balances, relating the particle velocities (u,v), the radial and circumferential stresses, and the density per unit volume (where α is the slope of the membrane with respect to the original plane) are:

$$\left. \begin{aligned} \Delta u &= \left\{ \sigma_r(i+1) \cdot r(i+1) \cos[\alpha(i+1)] - \sigma_r(i) r(i) \cos[\alpha(i)] \right. \\ &\quad \left. + \sigma_\theta(i) [r(i) - r(i+1)] \right\} 2 \Delta t / \rho [r^2(i+1) - r^2(i)], \\ \Delta v &= \left\{ \sigma_r(i+1) r(i+1) \sin[\alpha(i+1)] \right. \\ &\quad \left. - \sigma_r(i) r(i) \sin[\alpha(i)] \right\} 2 \Delta t / \rho [r^2(i+1) - r^2(i)]. \end{aligned} \right\} (5)$$

The radial (ϵ_r) and circumferential (ϵ_θ) strain-velocity relationships using the resultant particle velocity vector \bar{V} and radial particle velocity for an element length ΔR are:

$$\left. \begin{aligned} \Delta \epsilon_r(i) &= \frac{\bar{V}(i+1) - \bar{V}(i)}{\Delta R} \Delta t; & \Delta \epsilon_\theta(i) &= \frac{u(i) \Delta t}{r(i)}. \end{aligned} \right\} (6)$$

The stress-strain constitutive law using the tensile modulus (E) and Poisson's ratio (ν) is

$$\left. \begin{aligned} \Delta \sigma_r(i) &= \frac{E}{(1-\nu^2)} [\Delta \epsilon_r(i) + \nu \Delta \epsilon_\theta(i)] \\ \Delta \sigma_\theta(i) &= \frac{E}{(1-\nu^2)} [\nu \Delta \epsilon_r(i) + \Delta \epsilon_\theta(i)] \end{aligned} \right\} (7)$$

(Computations show that σ_θ would become negative. Therefore, a condition for buckling is stipulated. If σ_θ tries to go negative, σ_θ is set equal to zero in the constitutive relations above. In addition, the excess material (circumferentially) in the buckling zone (slack) is continually accounted for, and reloading must first take up the slack.)

Equations (5), (6), and (7) completely state the problem of traveling waves in an elastic, ideally flexible membrane allowing for circumferential buckling, when combined with appropriate initial conditions and boundary conditions.

In order to insure stability of these calculations the element size-time increment relation $\Delta t \geq \Delta R/C_0$ was used, where $C_0 = [E_0/\rho(1-\nu^2)]^{1/2}$ (E_0 is the highest value of tensile modulus corresponding to the strain magnitudes encountered in the deformation process).

RESULTS OF THE ANALYSIS

Transverse Impact of a Linear Elastic Filament

The following computations utilize a linear approximation of the stress-strain curve obtained by Smith⁴ for a high tenacity nylon yarn. The fiber studied by Smith appears to be quite similar to the high tenacity nylon yarn used in the experimental phase of the present work.¹

Figure 5 illustrates typical computed results for the longitudinal strain distribution at various times after impact in a linearly elastic fiber subjected to transverse impact. The reflection of waves at the boundary are automatically accounted for, simply by specifying the fixed boundary velocity to be zero. Note that there is an interaction between the longitudinal strain wave and the transverse filament deflection at approximately 110 μ sec which causes a certain percentage of the strain to continue propagating along the filament towards the impact point and eventually reflecting back again, and a certain percentage to be reflected back towards the fixed boundary as a tension pulse.

Figure 6 illustrates the transverse filament displacement history associated with the longitudinal strains described in Figure 5.

The above computations, even though based on an approximate linear stress-strain behavior, show remarkable agreement with the experimental results (such as those shown in Figure 1, for high tenacity nylon yarn). There is agreement on the shapes of the transverse displacement wave between Figure 1 and Figure 6. This is evident in the configurations of the filament after successive reflections of the transverse wave, as indicated in the 261 and 391 μ sec displays and the bend in the 130 μ sec curve at $X=2.5$ cm, which is caused by substantial differences in tension level across the longitudinal wave front at that position (see Figure 5). In addition there is quantitative agreement in the measured and predicted velocities of the leading edge of the transverse displacement wave and with the projectile energy losses discussed below.

Explanation of the Experimental Results for Projectile Energy Loss

An explanation of the experimental curve of projectile energy loss as a function of striking velocity in Figure 2 can be obtained by applying the above results to resolve the amount of kinetic and strain energy stored in

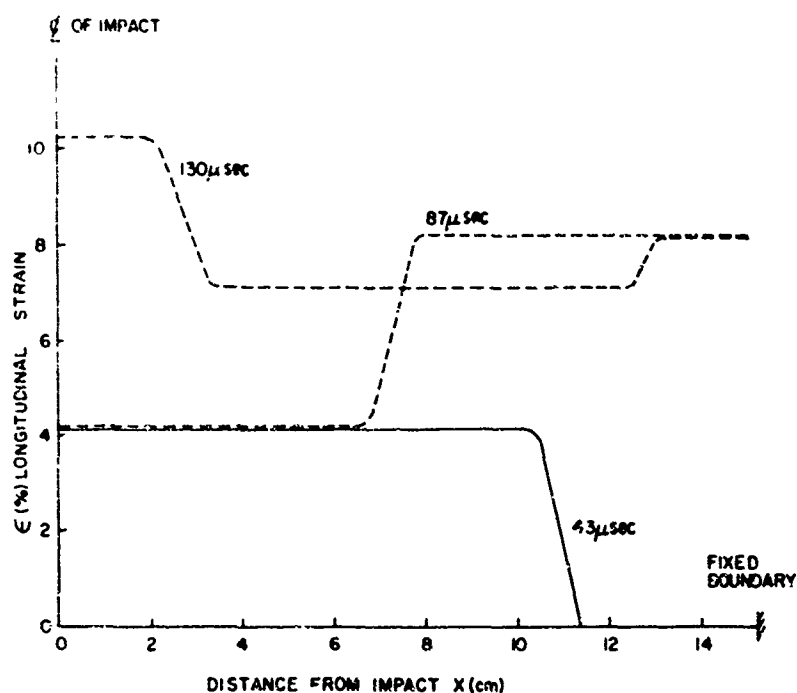


Figure 5. LONGITUDINAL STRAIN WAVE FOR VARIOUS TIMES AFTER IMPACT OF FILAMENT. Impact velocity = 334 meters/sec. Material: Linear approximation of high tenacity nylon of Ref. 4, E (modulus) = 80 grams/denier.

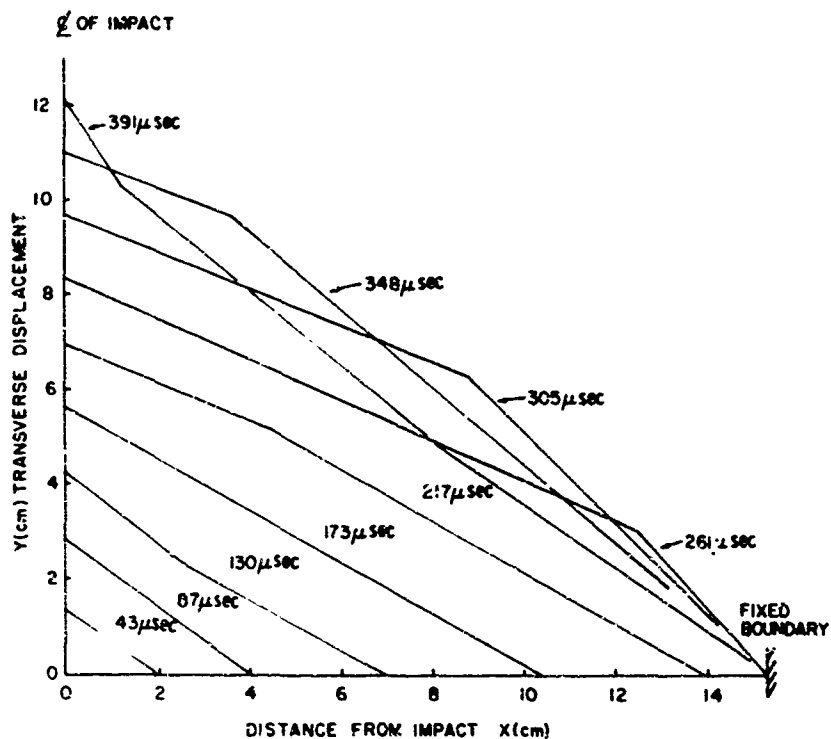


Figure 6. TRANSVERSE DISPLACEMENT OF FLEXIBLE FILAMENT VERSUS DISTANCE FROM IMPACT POINT FOR VARIOUS TIMES AFTER IMPACT. Impact velocity = 334 meters/sec. Material: Linear approximation of high tenacity nylon fiber of Ref. 4, E (modulus) = 80 grams/denier.

the fiber system. The shape of the curve is the result of either the strain energy or the kinetic energy of the fiber playing the dominant role at different impact velocities.

It is convenient to consider three velocity regimes over which the means of obtaining material properties and the manner in which the fiber-system responds (i.e., the importance of wave propagation effects and boundaries) are quite different:

Regime I corresponds to a quasi-static fiber deformation where multiple wave reflections have averaged out the velocity and strain fields and wave propagation effects are negligible. The material properties for these rates of deformation are most conveniently obtained by techniques outlined in Reference 3. The transverse velocity distributions are fairly linear from zero at the fixed boundary to the value of the projectile velocity at the impact point. At low velocities the kinetic energy of the fiber is negligible compared to the strain energy stored in the fiber at break. As the velocity approaches zero, the curve asymptotically approaches some breaking strain energy associated with the moderately high rates of loading experienced by the fibers in this regime. As the impact velocity increases, kinetic energy increases as the square of the velocity and becomes a major part of the energy stored in the fiber system.

Regime II corresponds to a truly dynamic system response in the sense that the wave-boundary interactions cause the peaking energy absorption effect shown in Figure 2. The material properties for these rates of deformation are most conveniently obtained by techniques outlined in Reference 4. A given impact velocity causes a specific amount of initial strain in a given fiber. The strain builds up, upon reflection (as illustrated in Figure 5), until the breaking strain is reached after a certain period of time. If this time corresponds to the time it takes for the transverse deflection wave to just reach the boundary (e.g., between 217 and 261 μsec in the situation illustrated in Figure 6), then the condition of maximum fiber kinetic energy (the entire fiber having a transverse velocity close to the impact velocity) and the condition of maximum strain energy coincide, giving rise to the peak energy absorption. At higher impact velocities the breaking strain is attained before the entire fiber is involved in transverse motion, so again the kinetic energy contribution drops off.

Regime III corresponds to a purely dynamic fiber response, in the sense that the initial strains are close to the breaking strains and the fiber breaks almost upon impact before any wave disturbance reaches the boundaries. Rate-dependent effects play a major role in the deformation mechanisms at these high rates. Considerations in Reference 5 and the appendix must be employed to arrive at a reasonable representation of the rate-dependent material behavior. Since less and less fiber is involved in deformation the energy absorbed decreases to zero.

Impact of Filament with Non-Linear Material Properties

Figure 7 illustrates typical results for the longitudinal strain distribution in a fiber with a non-linear stress-strain curve subjected to transverse impact. Comparison with analytical results of Smith, et al.,^{4,5} are also shown.

The initial steep wave front of the 1% strain is due to the fairly linear nature of the T- ϵ curve up to 1%. Note that the finite element solution (open circles) leads the analytical predictions because of a slightly higher value of initial modulus used in the finite element analysis. The curved portion is due to the gradual decrease of modulus with strain amplitude and the steep rise to the plateau is due to the linear nature of the T- ϵ curve at higher strain levels. There is also a slight dip in the T- ϵ curve which might mean that a weak shock wave has been formed in this steep rise to the plateau region.

Impact of Filament on Elastic Foundation

Figure 8 illustrates the longitudinal strain caused by transversely impacting a linear elastic fiber system backed up by an elastic foundation. The particular foundation stiffness chosen for illustration is quite high ($K=50,000$ grams/cm of fiber length/cm of deflection) and represents an extreme situation. The fiber properties are again the linear approximation of high tenacity nylon. Comparison should be made between Figure 8 and the results in Figure 5 for the same fiber, without backup, impacted at the same velocity. Experiments¹ have shown that the breaking strain for this fiber is approximately 12.5%. The strain concentrations (Figure 8) near the impact point, resulting from the restraining action of the foundation, cause the fiber to reach breaking strains after only 38 μ sec. The strain history in the fiber without backup in Figure 5 extends to only 130 μ sec after impact. Analysis of the subsequent strain history predicts that the breaking strain of 12.5% is attained after 230 μ sec and that the strain distribution along the fiber at that time is fairly uniform: $11\% \pm 1.5\%$. The average strain at break in the fiber is less than 4% (see Figure 8). Accordingly, the strain energy stored in the backed fiber is less than 15% of that stored in the fiber without a foundation. The kinetic energy of the backed fiber is also less than 15% of the unrestrained fiber kinetic energy at break since less than 2 cm of fiber is involved in transverse motion at 38 μ sec and the entire fiber is involved at 230 μ sec (see Figure 6).

This marked change in performance, when the deflection of the textile fiber is restricted, indicates that there is a need to study the consequences of the constraining effect of the body on the in-place armor system and that there might be a need to specify some deflection criteria for flexible armor systems.

This case also illustrates the versatility of the analysis to handle easily resistive forces which cause horrendous mathematical complexities in an analytical solution.

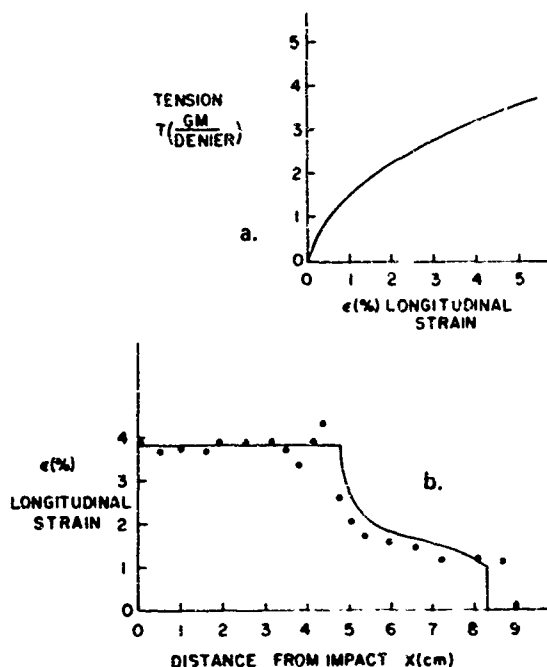


Figure 7. LONGITUDINAL STRAIN DISTRIBUTION IN A FIBER HAVING NON-LINEAR STRESS-STRAIN CURVE. a. Measured stress-strain curve for high tenacity polyester.⁵ b. Longitudinal strain distribution at 24 μ sec after impact and at an impact velocity of 308 M/sec. Finite element analysis $\circ \circ \circ$, analytical result—.

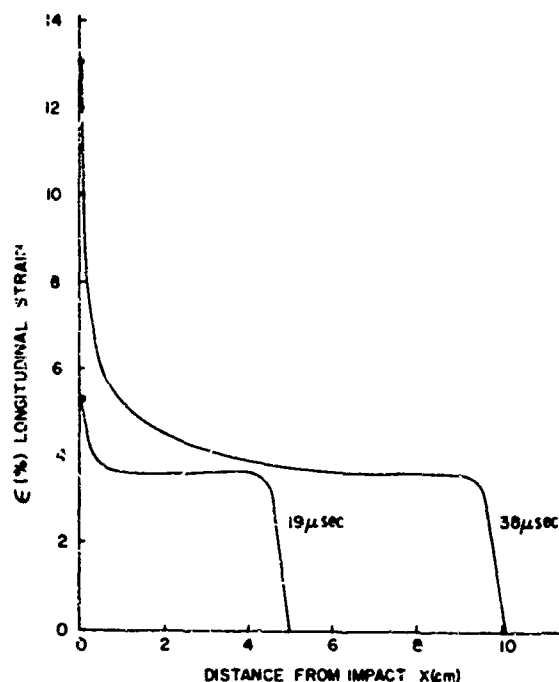


Figure 8. LONGITUDINAL STRAIN DISTRIBUTION PRODUCED BY THE IMPACT IN A FILAMENT SUPPORTED BY AN ELASTIC FOUNDATION. Material is the linear approximation of high tenacity nylon⁴ with $E = 80$ gm/denier. Impact velocity = 334 M/sec. Elastic foundation K (stiffness) = 50×10^3 gm/cm².

Transverse Impact of a Flexible Membrane

Figure 9 illustrates the radial and circumferential stresses produced in a membrane or 2-dimensional sheet of flexible material for various times after transverse impact.

Note that circumferential buckling occurs during the propagation of the stress waves prior to reflection at the boundaries. The buckling is caused by the fact that material is being fed into a smaller annular space at a rate which is faster than the buildup of radial tensile stress and the associated circumferential Poisson contraction which is required to take up this additional material.

The subsequent stress history, not illustrated here, predicts the effect of wave reflections from boundaries. The boundaries have a much less dramatic effect than they do in the fiber problem since the stress and strain amplitudes have decayed considerably with distance propagated. However, the reflected stress wave does bring the circumferential stress into tension.

This is the first rigorous model to be presented which can predict the transient deformation of a membrane subjected to transverse projectile impact.

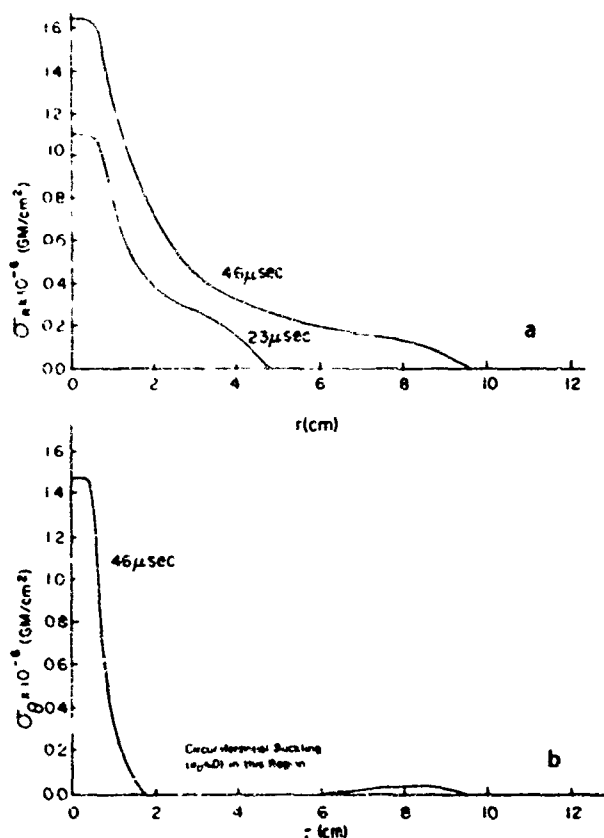


Figure 9. CALCULATED STRAIN DISTRIBUTION IN AN IMPACTED FLEXIBLE MEMBRANE USED AS AN APPROXIMATION TO THE RESPONSE OF A NYLON TEXTILE FABRIC. Nylon material properties: Young's modulus $E = 40 \times 10^6$ gm/cm²; Poisson's ratio $\nu = 0.35$; density $\rho = 1.15$ gm/cm³; thickness $\eta = 0.005$ cm. Impact velocity = 100 M/sec. a. Radial stresses versus radial distance from impact. b. Circumferential stress versus radial distance from impact.

CONCLUSIONS

A "finite element" mechanical model, capable of utilizing experimentally obtained material properties, has been developed for analyzing the behavior of a constrained fiber system when subjected to transverse impact.

The model has been applied successfully to the following transverse impact problems: (1) the prediction and interpretation of experimental results of transversely impacted finite lengths of nylon yarns rigidly clamped at both ends; (2) the impact of infinitely long fibers with non-linear material properties and the comparison of results with published theory; (3) predictions of strain concentrations caused by an elastic foundation transversely supporting a fiber subjected to impact; and (4) the transient deformation of an isotropic membrane subjected to projectile impact.

In view of the versatility of the finite element analysis, as indicated in the filament applications cited above, it appears reasonable to expect that further effort will yield improvements in modeling the physics of an actual fabric system and ultimately provide a viable model for predicting the response of the in-place anisotropic fabric or felt armor system subjected to transverse impact.

Appendix. LINEAR VISCOELASTIC EFFECTS

In the analyses outlined above, the material properties were assumed to be rate independent. In one of the latest papers by Smith⁵ the strain distribution along the fiber was measured experimentally. The marked differences illustrated in Figure A-1 between these results and the analytical results such as depicted in Figure 7 of the main text were attributed (according to an excellent physical argument) to viscoelastic effects.

The finite element model was, therefore, modified to accept a general type of stress relaxation modulus which can be expressed analytically as:

$$\tau(\bar{x}, t) = \int_0^t E(t-\tau) \frac{\partial \epsilon(\bar{x}, \tau)}{\partial \tau} d\tau \quad A1$$

This convolution integral was integrated by finite differences in order to be cast into a form amenable to the finite element model analysis following the procedure in Reference 8. Integrating the equation by finite differences in equal time increments $t(i)$ ($i=1,2,3,\dots,n+1$) where $t(1)=0$ and $t(n+1)=t$ and using the notation

$$\begin{aligned} T(n+1) &\equiv T(\bar{x}, t(n+1)) \\ \epsilon(J, n+1) &\equiv \epsilon(\bar{x}, t(n+1)) \\ E(n+1) &= E(t(n+1)) \end{aligned} \quad A2$$

the stress-strain relations become:

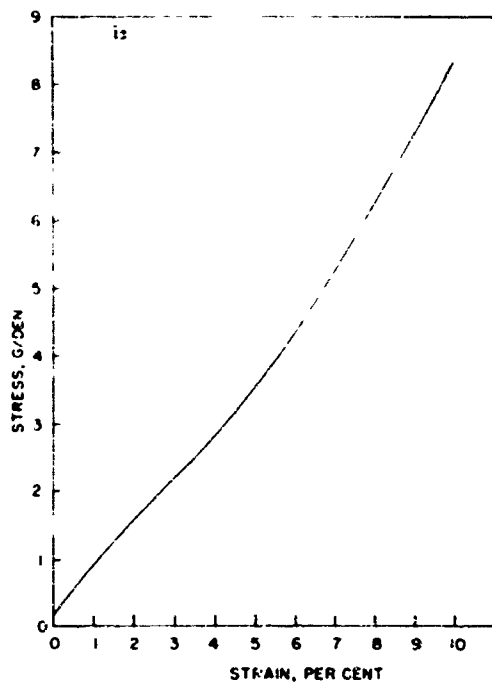
$$\begin{aligned} T(1) &= \epsilon(1) E(1) \\ T(2) &= \epsilon(2) \left\{ \frac{1}{2} [E(1) + E(2)] \right\} - \epsilon(1) \left\{ \frac{1}{2} [E(1) - E(2)] \right\} \\ T(n+1) &= \epsilon(n+1) \left\{ \frac{1}{2} [E(1) + E(2)] \right\} - \rho(n) \left\{ \frac{1}{2} [E(1) - E(3)] \right\} + \dots \\ &\quad - \epsilon(2) \left\{ \frac{1}{2} [E(n-1) - E(n+1)] \right\} - \epsilon(1) \left\{ \frac{1}{2} [E(n) - E(n+1)] \right\} \end{aligned} \quad A3$$

The only modification required in the analysis is to keep track of the strain history of each element $\epsilon(\bar{x}, n+1)$ and compute the current stress according to the above equations (A3).

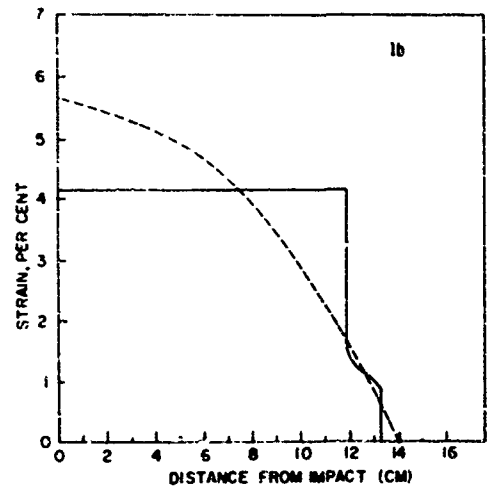
The problem of transversely impacting the linearly elastic filament as shown in Figure 5 was reconsidered, using a linear relaxation modulus varying from 100 gm/denier to 60 gm/denier in 40 μ sec as shown in the insert to Figure A-2.

Figure A-2 shows the results of the rate-independent finite element model vs the linear viscoelastic model. The particular relaxation time used was based on some of the qualitative arguments by Smith et al.⁵ The results qualitatively agree with the results of Smith et al illustrated in Figure A-1 and tend to prove his contention that there is a distinct relaxation process on the order of 50 μ sec in the subject nylon fiber.

A slight modification of the program to account for non-linear stress strain curves exhibiting relaxation behavior is now needed. These modifications, along with more judicious interpretation of the "rate-independent" moduli obtained by Smith et al.,⁴ should provide a model capable of predicting very accurately the detailed strain distribution (Figure A-1) in textile fibers caused by transverse impact.

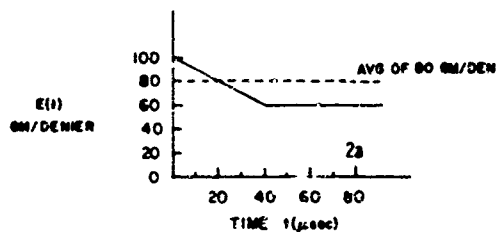


a. Stress-strain curve for high tenacity nylon.

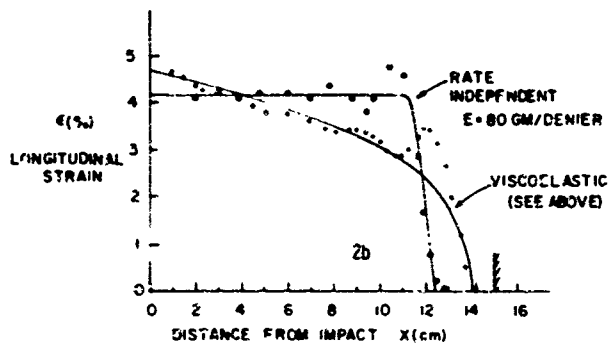


b. Rate-independent prediction obtained from stress-strain curve (solid line). Experimentally measured strain distribution (dashed line)

Figure A-1. COMPARISON OF LONGITUDINAL STRAIN IN FILAMENT SUBJECTED TO TRANSVERSE IMPACT CALCULATED FROM RATE-INDEPENDENT THEORY AND MEASURED EXPERIMENTALLY⁵



a. Linear relaxation model representing a viscoelastic approximation of high tenacity nylon.⁵



b. Strain distribution obtained from rate-independent theory and from the viscoelastic approximation (curve represents the experimental behavior depicted in A-1b).

Figure A-2. LONGITUDINAL STRAIN IN VISCOELASTIC FILAMENT SUBJECTED TO TRANSVERSE IMPACT

LITERATURE CITED

1. Wilde, A. F., Ricca, J. J., Cole, L. M., and Rogers, J. M. "Dynamic Response of a Constrained Fibrous System Subjected to Transverse Impact. Part I, Transient Responses and Breaking Energies of Nylon Yarns." AMMRC Technical Report, in process.
2. Smith, J. C. et al, Textile Research J., v28, 288-302 (1958)
3. Smith, J. C. et al, Textile Research J., v31, 721-734 (1961)
4. Smith, J. C. et al, Textile Research J., v33, 919-933 (1963)
5. Smith, J. C. et al, Textile Research J., v35, 743-747 (1965)
6. Mehta, and Davids, AIAA J., v4, 112-117 (1966)
7. Koenig, and Davids, Intl J. of Solids & Structures, v4, 643 (1968)
8. Lynch, F. deS., Intl J. for Numerical Methods in Engrg, v1, 379-394 (1969)

UNCLASSIFIED
Security Classification

DOCUMENT CONTROL DATA - R & D		
Security classification of title, body of abstract and indexing annotation must be entered when the overall report is classified		
1. ORIGINATING ACTIVITY (Corporate author) Army Materials and Mechanics Research Center Watertown, Massachusetts 02172		2a. REPORT SECURITY CLASSIFICATION Unclassified
		2b. GROUP
3. REPORT TITLE DYNAMIC RESPONSE OF A CONSTRAINED FIBROUS SYSTEM SUBJECTED TO TRANSVERSE IMPACT. PART II: A MECHANICAL MODEL		
4. DESCRIPTIVE NOTES (Type of report and inclusive dates)		
5. AUTHOR(S) (First name, middle initial, last name) Francis deS. Lynch		
6. REPORT DATE July 1970	7a. TOTAL NO. OF PAGES 18	7b. NO. OF REFS 8
8a. CONTRACT OR GRANT NO. b. PROJECT NO D/A 1T062105A329 c. AMCMS Code 502E.11.295 d. Agency Accession Number DA OB 4752		9a. ORIGINATOR'S REPORT NUMBER(S) AMMRC TR 70-16
		9b. OTHER REPORT NO(S) (Any other numbers that may be assigned this report)
10. DISTRIBUTION STATEMENT This document has been approved for public release and sale; its distribution is unlimited.		
11. SUPPLEMENTARY NOTES		12. SPONSORING MILITARY ACTIVITY U. S. Army Materiel Command Washington, D. C. 20315
13. ABSTRACT A "finite element" mechanical model, capable of utilizing experimentally determined material properties, is presented for analyzing the deformation processes in a <u>finite, constrained flexible filament</u> subjected to transverse impact. The model is then used to analyze the results of experimentally (transversely) impacted finite lengths of nylon yarns rigidly clamped at both ends. The experimental analysis is presented in Part I of this work. The analysis is used to determine the effects of an elastic foundation transversely supporting a flexible filament subjected to transverse impact. Finally, results of a finite element analysis of a transversely impacted isotropic membrane are presented to indicate the direction for future research. An appendix is attached which demonstrates the ability to include rate-dependent material properties in the analyses described above. (Author)		

DD FORM 1473

REPLACES DD FORM 1473, 1 JAN 64, WHICH IS
OBSOLETE FOR ARMY USE.

UNCLASSIFIED
Security Classification

KEY WORDS	LINK A		LINK B		LINK C	
	ROLE	WT	ROLE	WT	ROLE	WT
Textiles Nylon fibers Numerical analysis Mechanical properties Impact Deformation Body armor Lightweight armor						